

## Positive-Energy Spectrum of the Hydrogen Atom in a Magnetic Field

D. Delande, A. Bommier, and J. C. Gay

*Laboratoire de Spectroscopie Hertzienne de l'École Normale Supérieure, 4, place Jussieu,  
Tour 12-E1, 75252 Paris CEDEX 05, France*

(Received 31 October 1990)

The positive-energy spectrum of the hydrogen atom in a magnetic field is deduced by making use of the complex-rotation method combined with Stürmian-type expansions. This yields the energies and widths of the resonances especially for fields of atomic interest. Accidental destructive interference generates ultranarrow resonances above the ionization threshold as experimentally observed.

PACS numbers: 32.60.+i, 05.45.+b, 31.50.+w

The hydrogen atom in a magnetic field has become recognized as a prototype for the study of nonintegrability in a system which is experimentally accessible. The problem has attracted considerable attention with respect to the study of quantum manifestations of classical chaos.<sup>1</sup>

High-quality experimental results on hydrogen<sup>2</sup> and alkali-metal atoms<sup>3</sup> have stimulated the theoretical analysis of the bound discrete spectrum, yielding accurate predictions of the positions and intensities of the lines and revealing numerous features that are characteristic of nonintegrability in the structure of the eigenstates.<sup>4</sup> Recent experimental investigations of the positive-energy spectrum of lithium with 30-MHz resolution have revealed new phenomena<sup>3</sup> which dramatically demonstrate that the positive-energy limit of the system is not yet understood. This Letter presents the first numerical simulations of the positive-energy spectrum that can yield accurate results at laboratory field strengths ( $B \approx 6$  T), allowing us to interpret some of the experimental findings.

The Hamiltonian of the atom in a magnetic field (along the  $z$  axis) is (atomic units)

$$H = \frac{p^2}{2} - \frac{1}{r} + \frac{\gamma}{2} l_z + \frac{\gamma^2}{8} \rho^2. \quad (1)$$

$l_z$ , the  $z$  component of the angular momentum, is a constant and  $\gamma = B/B_c$  ( $B_c = 2.35 \times 10^5$  T). The proton mass is assumed infinite.

Asymptotically, the Hamiltonian (1) tends to the Landau Hamiltonian with ionization thresholds:

$$E_N = (N + \frac{1}{2})\gamma, \quad (2)$$

where  $N$  is a non-negative integer that labels the Landau levels. The Coulomb potential induces a coupling between the Landau channels. At high fields ( $\gamma \gg 1$ ), adiabatic separation of the slow motion along  $B$  yields the picture of an infinite set of Landau thresholds each supporting a quasi-one-dimensional Rydberg progression. Because of the coupling with the continua of the lower Landau levels, all these series, except for the lowest one which is discrete, are composed of resonances with

nonzero autoionizing widths. At lower fields ( $\gamma < 1$ ), such an adiabatic separation cannot be expected to apply.

As noted by a number of authors,<sup>5-7</sup> the complex-coordinate method is well suited for analyzing such a situation. This amounts to making the replacements  $\mathbf{r} \rightarrow \mathbf{r}e^{i\theta}$ ,  $\mathbf{p} \rightarrow \mathbf{p}e^{-i\theta}$  in the Hamiltonian (1), yielding

$$H(\theta) = \frac{p^2}{2} e^{-2i\theta} - \frac{e^{-i\theta}}{r} + \frac{\gamma}{2} l_z + \frac{\gamma^2}{8} \rho^2 e^{2i\theta}. \quad (3)$$

The rotated Hamiltonian  $H(\theta)$  ( $0 \leq \theta \leq \frac{1}{4}\pi$ ) is non-Hermitian with a complex spectrum characterized by the following key properties (mathematical proofs can be found in Refs. 5-7), with reference to  $H = H(\theta=0)$ : (i) The continua are rotated by the angle  $2\theta$  into the lower half plane around their branch points (the Landau thresholds); (ii) the bound (discrete) spectra of  $H(\theta)$  and  $H$  coincide below the first Landau threshold; (iii) The resonances of  $H$  coincide with the complex eigenvalues of  $H(\theta)$ . The real part (the energy) and the imaginary part (negative of the half-width) are  $\theta$  independent provided that the rotation of the continua has uncovered the resonances.

Another key property in the method is that the resolvent operator of  $H$  can be expanded onto eigenstates of the rotated Hamiltonian in a finite region near the nucleus. Although this seems like a straightforward use of analyticity properties, the nonunitary character of the complex dilatation causes  $H(\theta)$  to be non-Hermitian, giving this expansion an unusual character. In a basis of real functions, the matrix of  $H(\theta)$  is complex symmetrical, and the eigenvectors  $|\varphi_i(\theta)\rangle$  are nonorthogonal. The left eigenvectors  $|\varphi_i(\theta)\rangle^T$  are the transposed values of  $|\varphi_i(\theta)\rangle$ , not the Hermitian conjugates, and they are normalized so that  $|\varphi_i(\theta)\rangle^T |\varphi_j(\theta)\rangle = \delta_{ij}$ . This leads to the biorthogonal spectral expansion:<sup>5</sup>

$$H(\theta) = \sum_i E_i(\theta) |\varphi_i(\theta)\rangle |\varphi_i(\theta)\rangle^T, \quad (4)$$

where the sum is over all discrete and continuous states, and  $E_i(\theta)$  are the eigenvalues of  $H(\theta)$ .

The cross section for photoionization  $\sigma(\omega)$  from the

discrete state  $|\psi_0\rangle$  with energy  $E_0$  is given by<sup>7</sup>

$$\sigma(\omega) = \frac{4\pi\omega}{c} \text{Im} \langle \psi_0 | T \frac{1}{H - \omega - E_0 - i\epsilon} T | \psi_0 \rangle, \quad (5)$$

where  $T = \mathbf{e} \cdot \mathbf{r}$  is the dipole operator for polarization  $\mathbf{e}$ . The matrix element can be reexpressed as  $\{|\psi\rangle^T [H(\theta) - \omega - E_0]^{-1} |\psi\rangle\}$  by introducing the complex rotation.<sup>7</sup> Here  $|\psi\rangle$  is the complex-rotation transform of  $T|\psi_0\rangle$ , which we can further expand on the eigenvectors of  $H(\theta)$  as  $\sum c_i(\theta) |\varphi_i(\theta)\rangle$ . Finally,

$$\sigma(\omega) = \frac{4\pi\omega}{c} \text{Im} \sum_i \frac{c_i^2(\theta)}{E_i(\theta) - \omega - E_0} \quad (6)$$

The photoionization cross section is now the sum of *well isolated* contributions arising from the eigenspectrum of the rotated Hamiltonian; it is free from the divergences in Eq. (5). An isolated resonance leads to a Beutler-Fano profile whose detailed shape depends on  $\text{arg} c_i$

A Sturmian basis<sup>8</sup> is well suited to diagonalizing the rotated Hamiltonian. Such a complete and discrete basis complies with the dynamical group  $SO(4,2)$  of the hydrogen atom<sup>9</sup> and its oscillator representation (whose eigenbasis is precisely a Sturmian basis). The matrix elements have a known analytical form. As a result of selection rules, the complex symmetrical matrix of  $H(\theta)$  is banded with few nonzero elements. Studies of the bound spectrum<sup>1,9</sup> have revealed the outstanding efficiency of the method. Its natural extension to the positive-energy spectrum again leads to a generalized eigenvalue problem, but for a complex symmetrical banded matrix. Here, the diagonalization of  $H(\theta)$  has been

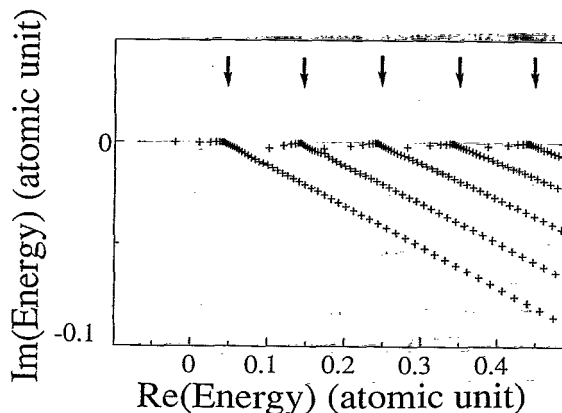


FIG. 1. Spectrum of the rotated Hamiltonian  $H(\theta)$  [Eq. (3)] obtained from the Hamiltonian of the hydrogen atom in a magnetic field [Eq. (1)] through a dilatation transformation  $\mathbf{r} \rightarrow \mathbf{r}e^{i\theta}$ . The continua rotate around the Landau thresholds, exposing the resonances (crosses) as complex eigenvalues.  $H(\theta)$  is truncated and diagonalized in a finite basis, and the continua appear as sets of discrete eigenvalues lying approximately on straight lines (diagonalization of a  $10000 \times 10000$  complex symmetrical matrix:  $\gamma=0.1$ ;  $l_z=0$ , odd-parity spectrum;  $\theta=0.1$ ). The arrows indicate the successive Landau thresholds [Eq. (2)].

performed using a stable implementation of the Lanczos algorithm.<sup>10</sup>

Figure 1 displays the complex energy spectrum of  $H(\theta)$  for  $\gamma=0.1$ . The field,  $2.35 \times 10^4$  T, is too high to be realized in the laboratory, but the calculation allows us to check our results against previous work.<sup>11,12</sup> As expected, the spectrum is composed of resonances whose positions are independent of  $\theta$  and of continua rotated by  $-2\theta$  around the Landau thresholds. The associated photoionization spectrum from the ground state is shown in Fig. 2. Two quasi-1D Rydberg progressions leading to Fano-shaped profiles and converging to the second and third Landau thresholds are exhibited. Except in the immediate vicinity of the thresholds (see below), these calculations are fully converged. This has been checked by varying the size of the truncated basis, the angle of rotation  $\theta$ , and the parameter (the real part of the dilatation) of the Sturmian basis. An additional "blind" check of the overall reliability can be obtained by noting that between the first and the second Landau thresholds, there is only one open channel for ionization. This implies that destructive interference between neighboring resonances should cause exact cancellation of the cross section for some energies. Our fully converged numerical calculations agree well with these predictions, while nonconverged calculations could lead incorrectly to negative cross sections.

A drawback to our method comes from the unavoidable truncation of the Sturmian basis. This manifests itself in Fig. 1 in the rotated continua appearing as sets of discrete eigenvalues lying approximately on straight lines. Provided the energy spacing between two consecutive members of the set is smaller than their widths, this will have no consequence on the photoionization cross

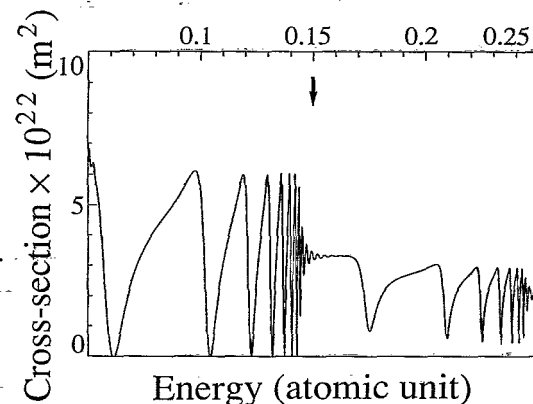


FIG. 2. Numerical simulation of the photoionization cross section of the hydrogen atom in a magnetic field ( $\gamma=0.1$ ;  $l_z=0$ , odd-parity series; ionization from the ground state with a laser polarization along the magnetic field). The Rydberg series converging to the Landau thresholds are clearly visible. Note the null values of the cross section below the second Landau level and the Fano-shaped profiles (the data are those of Fig. 1).

section and linewidths of the resonances. Overlapping of the various contributions will simulate a real continuum. This fails only in the vicinity close to the Landau thresholds where the imaginary parts are small, but the reproduction of the infinite number of oscillations of a Rydberg series at threshold is obviously impossible using a finite basis.<sup>11,12</sup>

The method, in contrast to previous ones, can be extended to lower fields (that are experimentally relevant), where the adiabatic approach becomes poor due to the strong interactions between the 1D Rydberg series. Here, the Rydberg series cannot be identified except in some narrow windows (see Ref. 3 and the following Letter<sup>13</sup>). By increasing the sizes of the basis to 62 500, the positions and widths of the resonances at  $B=6$  T are usually reproduced to high accuracy,  $\approx 5 \times 10^{-10}$  a.u. (i.e.,  $10^{-4}$  cm<sup>-1</sup>), which is 1 order of magnitude better than the experimental results available.<sup>3</sup> However, for a few broad resonances, the uncertainty on the position can be slightly larger, of the order of  $10^{-3}$  cm<sup>-1</sup>. The mean spacing between two consecutive resonances is of the order of  $4 \times 10^{-2}$  cm<sup>-1</sup>. Spurious shifts in the ionization thresholds and questions of convergence in their vicinity can be investigated and controlled by locally changing the size and parameter of the basis.

Figure 3 displays the photoionization spectrum from the 3s state between +6 and +8 cm<sup>-1</sup> at  $\gamma=2.595 \times 10^{-5}$  ( $B=6.10$  T), which looks similar to the experimental spectrum of lithium<sup>3</sup> (a detailed comparison is performed in the following Letter<sup>13</sup>). Broad resonances (width  $\approx 10^{-1}$  cm<sup>-1</sup>) coexist with narrow ones, for example, of a width  $8 \times 10^{-4}$  and  $1.4 \times 10^{-4}$  cm<sup>-1</sup> near  $E = +6.40$  cm<sup>-1</sup>. Upon small changes of  $\gamma$ , the narrow lines broaden while others become narrower. This agrees with the experimental observations of lithium.<sup>3</sup>

Sharp levels at positive energy occur because of the in-

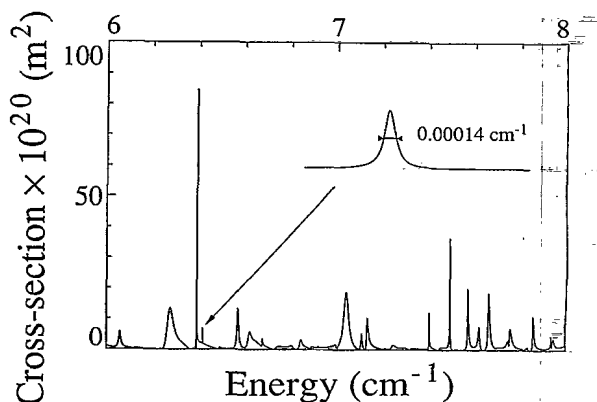


FIG. 3. Numerical simulation of the photoionization cross section from the 3s state in a field of 6.10 T ( $\gamma=2.595 \times 10^{-5}$ ). Two very narrow lines between +6 and +8 cm<sup>-1</sup> are visible near  $E = +6.4$  cm<sup>-1</sup> (diagonalization of a  $62\,500 \times 62\,500$  matrix).

teraction of several discrete states (associated with excited Landau levels) with a single continuum of ionization (between the first and second Landau thresholds). Each discrete state is coupled to the continuum by a real matrix element, the square of which is proportional to the width of the resonance. Upon accidental cancellation of this matrix element, the discrete state becomes a bound state embedded in the continuum.<sup>12</sup> It is well known that such a cancellation is likely to take place when two discrete states interact with each other (anticross) and with a continuum. For a specific value of  $\gamma$ , close to the anticrossing point, one state is stabilized and becomes a bound state.<sup>14</sup> This is the origin of narrow resonances in the present spectrum.

Refinements to the previous model would take into account the chaotic character of the dynamics. This means that all the discrete states should have complicated anticrossings associated with level repulsion and that the eigenstates vary rapidly with  $\gamma$ . The matrix elements for ionization should exhibit strong fluctuations and in the ideal case of a random-matrix-theory model, Gaussian fluctuations around zero. The most probable width should then be zero.

Such a stabilization has already been observed numerically at much higher magnetic fields<sup>12</sup> ( $\gamma \approx 1$  where the adiabatic approximation applies) as well as in other external field situations.<sup>14</sup> Above the second Landau threshold, observing narrow resonances requires that two real matrix elements be simultaneously small, which is less probable.

Finally, we note that the periodic-orbit analysis developed to interpret the bound spectrum<sup>1</sup> can be extended to a continuous spectrum. This is demonstrated in Fig. 4 where Fourier transforms for the bound and positive

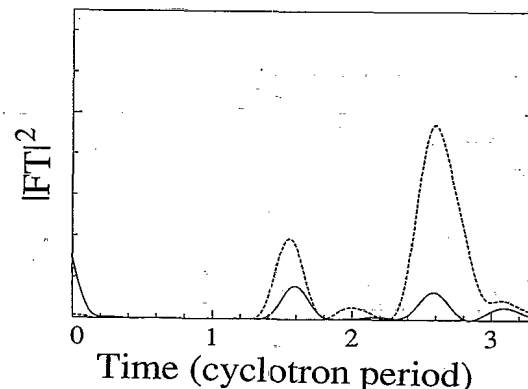


FIG. 4. Squared Fourier transform of the fluctuating part of the photoionization cross section (Welch windowing) from the 3s state in a field of 6.114 T ( $\gamma=2.601 \times 10^{-5}$ ): Energy interval  $[-30$  cm<sup>-1</sup>;  $0$  cm<sup>-1</sup>] (dotted line); energy interval  $[0$  cm<sup>-1</sup>;  $30$  cm<sup>-1</sup>] (solid line). In the two spectra, which are of very different nature (discrete and continuous), the peaks associated with periodic orbits are clearly visible (diagonalization of a  $22\,500 \times 22\,500$  matrix).

spectrum are compared. They display the same peaking at periodic orbits.

The method described here provides an important new tool for the quest to understand nonseparable quantum systems and the quantum manifestations of classical chaos.

We thank R. Niemeier and G. Wunner for providing us with useful references on the Lanczos algorithm. We acknowledge support from Département de Physique de l'École Normale Supérieure. CPU time on the Cray 2 computer has been provided by the Conseil Scientifique du Centre de Calcul Vectoriel pour la Recherche. Laboratoire de Spectroscopie Hertzienne de l'École Normale Supérieure et de l'Université Pierre et Marie Curie is Unité Associée No. 18 du Centre National de la Recherche Scientifique.

<sup>1</sup>See, for example, H. Friedrich and D. Wintgen, *Phys. Rep.* **183**, 37 (1989); H. Hasegawa, M. Robnik, and G. Wunner, *Prog. Theor. Phys.* **98**, 198 (1989); in *Atomic Spectra and Collisions in External Fields*, edited by M. H. Nayfeh, C. W. Clark, and K. T. Taylor (Plenum, New York, 1989), Vol. 2.

<sup>2</sup>A. Holle, G. Wiebusch, J. Main, B. Hager, H. Rottke, and K. H. Welge, *Phys. Rev. Lett.* **56**, 2594 (1986); J. Main, G. Wiebusch, A. Holle, and K. H. Welge, *Phys. Rev. Lett.* **57**, 2789 (1986); A. Holle, J. Main, G. Wiebusch, H. Rottke, and K. H. Welge, *Phys. Rev. Lett.* **61**, 161 (1988).

<sup>3</sup>G. R. Welch, M. M. Kash, C. Iu, K. Hsu, and D. Kleppner,

*Phys. Rev. Lett.* **62**, 893 (1989); **62**, 1975 (1989); C. Iu, G. R. Welch, M. M. Kash, K. Hsu, and D. Kleppner, *Phys. Rev. Lett.* **63**, 1133 (1989).

<sup>4</sup>D. Delande and J. C. Gay, *Phys. Rev. Lett.* **59**, 1809 (1987); D. Wintgen and A. Hönig, *Phys. Rev. Lett.* **63**, 1467 (1989).

<sup>5</sup>S. I. Chu, *Chem. Phys. Lett.* **58**, 462 (1978); S. K. Bhattacharya and S. I. Chu, *J. Phys. B* **16**, L471 (1983); A. Bomnier, Magistère Diploma, University Paris 6, 1989 (unpublished); A. Maquet, S. I. Chu, and W. P. Reinhardt, *Phys. Rev. A* **27**, 2946 (1983).

<sup>6</sup>E. Balslev and J. M. Combes, *Commun. Math. Phys.* **22**, 280 (1971).

<sup>7</sup>J. M. Rescigno and V. McKoy, *Phys. Rev. A* **12**, 522 (1975).

<sup>8</sup>D. Delande and J. C. Gay, *J. Phys. B* **17**, L335 (1984).

<sup>9</sup>D. Delande and J. C. Gay, *Phys. Rev. Lett.* **57**, 2006 (1986).

<sup>10</sup>T. Ericsson and A. Ruhe, *Math. Comp.* **35**, 1251 (1980), and references therein.

<sup>11</sup>A. Alijak, J. Hinze, and J. T. Broad, *J. Phys. B* **23**, 45 (1990); M. Vincke and D. Baye, *J. Phys. B* **20**, 3335 (1987); C. H. Greene, *Phys. Rev. A* **28**, 2209 (1983).

<sup>12</sup>H. Friedrich and M. Chu, *Phys. Rev. A* **28**, 1423 (1983); H. Friedrich and D. Wintgen, *Phys. Rev. A* **31**, 3964 (1985).

<sup>13</sup>Chun-ho Iu, G. R. Welch, M. M. Kash, D. Kleppner, D. Delande, and J. C. Gay, following Letter, *Phys. Rev. Lett.* **66**, 145 (1991).

<sup>14</sup>J. Y. Liu, P. McNicholl, D. A. Harmin, J. Ivri, T. Bergeman, and H. J. Metcalf, *Phys. Rev. Lett.* **55**, 189 (1985); S. Feneuille, S. Liberman, E. Luc-Koenig, J. Pinard, and A. Taleb, *J. Phys. B* **15**, 1205 (1982).